Scattering Functions of Flexible Polyelectrolytes in the Presence of Mixed Valence Counterions: Condensation and Scaling

Jérôme Combet,* François Isel, and Michel Rawiso

Institut Charles Sadron (CNRS-ULP), 6 rue Boussingault, 67083 Strasbourg Cedex, France

François Boué

Laboratoire Léon Brillouin (CEA-CNRS), CE Saclay, 91191 Gif-sur-Yvette Cedex, France

Received October 1, 2004; Revised Manuscript Received June 3, 2005

ABSTRACT: We have investigated by small-angle X-ray and neutron scattering the structure of salt-free aqueous solutions of sulfonated polystyrene with variable fractions of monovalent (sodium, Na) and divalent (calcium, Ca) counterions. We follow the variation of the position of the maximum in the scattered intensity, q^*, as a function of the concentration, c, and the fraction of Ca counterions. A relevant parameter is the degree of condensation of Na and Ca counterions in the different mixtures. We survey the literature and check that, in the case of monovalent counterions, the variation of q^* with c can be described by the scaling theory of Dobrynin, Colby, and Rubinstein, provided the counterion condensation is included according to the Manning−Oosawa approach. Scattering data from mixed valence systems are still in agreement with this scaling model at lower concentrations, except for pure $CaPSS_2$ aqueous solutions. For increasing concentration, a discrepancy is enhanced that extends toward higher Ca fractions. This indicates that counterion condensation is not the only process. Another possible one is a retraction of the macroions due to divalent counterions that induce bridging-type correlations between monomers, as already observed on the form factors of $CaPSS_2$ and NaPSS plus added $CaCl_2$ salt. Such a retraction modifies the scaling, in particular, via a change in the overlap concentration c^*. Furthermore, it is noticeable that q^* measurements have to be handle with care. We show that misinterpretation of the characteristic maximum in the small-angle scattering of polyelectrolyte solutions may occur, especially at high concentration, if the contribution of the condensed counterions to the total scattering function is predominant.

1. Introduction

Polyelectrolytes are ionic polymers which, when dissolved in a polar solvent such as water, dissociate into macroions and small mobile counterions. Electrostatic charges of one sign are localized on the macroions whereas an equivalent amount of oppositely charged counterions is either condensed onto the macroions or scattered in the solution. Because of their relevance in biology as well as in technological applications, increasing attention has been paid to these charged polymers.[1−6] The understanding of their properties is, however, far from complete. When dissolved in a good solvent (hydrophilic polyelectrolytes), their properties are more complex than those of neutral polymers because electrostatic interactions are long-ranged. In a poor solvent (hydrophobic polyelectrolytes), the complexity results from the competition between the long-range electrostatic repulsions and the short-range attractions associated with the poor solubility.

But other degrees of freedom are brought by counterions that can also play a crucial role with respect to interactions. Numerous experiments[6−19] as well as simulations[6,20−25] and theories[6,26−39] have shown that like-charged macroions can attract each other through effective forces of electrostatic origin. Contrarily to the usual electrostatic repulsions, such attractive interactions are short-ranged. They also require the presence of multivalent counterions, or small ions of the opposite sign, in the solutions. For linear macroions, they lead to distinct aggregated structures according to their length and/or their stiffness. For rigid macroions, it is the formation of dense or ordered packages, as bundles for DNA condensates, that tend to form a network superstructure, which is observed; for flexible macroions, it is rather a retraction in the average conformation or the formation of compact precipitates or macroscopic physical gels, which is observed. Therefore, the origin of multivalent counterion-mediated attractions between like-charged chains, or monomers, is presumably different in both cases. It is the existence of diffuse electrostatic correlations among condensed counterions that induce the formation of bundles, whereas the precipitation of linear flexible polyelectrolytes in multivalent salts is attributed to the bridging of monomers via multivalent ions associated with more than one monomer.

In this paper we wish to follow step by step the effect of the counterion valence on the structure of a given highly charged flexible polyelectrolyte. To consider only electrostatic effects, our system will not involve any complexation (chemical bonding) between macroion and counterions. This is the case for sulfonated polystyrene (PSS) linear macroions with sodium (Na) and/or calcium (Ca) counterions.[14] The static structure of their semidilute aqueous solutions is investigated here using small-angle X-ray and neutron scattering (SAXS and SANS) techniques.

SANS experiments have already been devoted to solutions of that kind.[16,17] They show first that the characteristic broad maximum in the scattering function is shifted toward smaller scattering vectors, when

* Corresponding author: Tel +33 3 88 41 40 96; Fax +33 03 88 41 40 99; e-mail combet@ics.u-strasbg.fr.

10.1021/ma0479722 CCC: $30.25
Published on Web 07/21/2005

monovalent (Na) counterions are replaced by divalent (Ca) ones. Correlatively, the average size of the macroions is found to be smaller in the presence of Ca counterions. Two distinct interpretations were proposed. On one hand, a decrease in the effective charge fraction associated with the counterion condensation process[40,41] was invoked;[16] on the other hand, a conformational change resulting from an electrostatic bridging between monomers by Ca counterions was considered.[17] The second explanation was obviously inspired by previous investigations on complexation between weak polyelectrolytes and divalent counterions.[9,14] It is also strengthened by some numerical simulations on short macroions.[25,42] However, both interpretations are reasonable since the experimental results cannot really distinguish between them.

To settle this problem, we intend to take SAXS and SANS experiments up on more suitable systems, namely salt-free aqueous solutions of PSS with mixtures of Na and Ca counterions of variable ratios. Such mixed valence systems have actually been studied in the past.[43−47] We will see that they allow more specifically to distinguish condensed counterions from free counterions and therefore to establish their respective real roles in attractive interactions between monomers when these counterions are divalent. For the sake of simplicity, scattering data will be analyzed in the framework of the scaling theories[48−50] combined with the counterion condensation concept. More precisely, the validity of such an approach will be challenged for each of the mixed valence systems and studied according to the concentration in the semidilute regime.

The rest of the paper is organized as follows: In section 2, we will describe all the experimental details and present the main characteristics of the investigated PSS samples as well as the ones of other systems extracted from literature for which particular attention will be paid. In section 3, we will present SAXS and SANS results obtained from salt-free aqueous solutions of Na−CaPSS. Section 4 will be devoted to the Manning−Oosawa approach of the counterion condensation process and the scaling theory of Dobrynin, Colby, and Rubinstein. We will demonstrate that a combination of these models is able to describe the static structure of salt-free aqueous solutions of flexible polyelectrolytes in the presence of monovalent counterions. At last, in section 5, we will focus on the mixed valence systems, and comparison with the previous theoretical models will be carried out in order to elucidate the respective roles of monovalent (Na) and divalent (Ca) counterions, as well as the ones of the free and condensed counterions.

2. Experimental Methods

2.1. Materials. Hydrogenated and deuterated polystyrene (PS) chains with a narrow molecular weight distribution were synthesized by anionic polymerization and then sulfonated according to the Makowski et al. procedure.[51−55] After neutralization with either sodium hydroxide (NaOH) or calcium hydroxide ($CaOH_2$), and tetramethylammonium hydroxide (TMAOH) for deuterated chains, sodium (respectively calcium and tetramethylammonium)-sulfonated polystyrene (NaPSS, $CaPSS_2$, and $TMAPSS_d$) chains were purified by extended dialysis against pure water (conductivity of the order of 1 μS) and obtained in powder after freeze-drying (note that $CaPSS_2$ and $TMAPSS_d$ macromolecules are only labeled CaPSS and TMAPSS hereafter). Their characterization was carried out by elemental analysis. In this way, the degree of sulfonation τ_s, defined as the ratio of sulfonated monomers to the total number of monomers, and the weight fraction of water content τ_w were determined for each sample. The molecular weights of the parent PS polymer samples (before sulfonation) were characterized by size exclusion chromatography (SEC). Table 1 lists the main characteristics of these samples.

Table 1. Characteristics of Polystyrene and Sulfonated Polystyrene Samples[a]

	M_n (g/mol)	N_n	I	τ_s	τ_w
NaPSS	77 600	745	1.04	0.90	0.07
CaPSS	77 600	745	1.04	0.90	0.07
TMAPSS	82 200	733	1.16	1.00	0.10

[a] M_n and N_n are the number-average molecular weights and the number-average degrees of polymerization of the parent PS macromolecules ($N_n = M_n/m$; m is the molar mass of PS monomers (104.15 g/mol for PS_h and 112.20 g/mol for PS_d)); I is their polydispersity index. These characteristics have been obtained from SEC measurements, by using THF as eluent and a low-angle laser light scattering spectrometer (LALLS; down DSP) as molecular mass detector. τ_s and τ_w are the degree of sulfonation and the weight fraction of water content of the related dried Na, Ca, and TMAPSS polyelectrolytes, respectively. Such characteristics are obtained from elemental analysis. Specifically, they allow to determine the concentrations (mol/L) of the various aqueous solutions.

The salt-free aqueous solutions of Na−CaPSS were obtained by dissolving NaPSS and CaPSS chains in ultrapure H_2O (Millipore grade, conductivity < 1 μS) for X-ray scattering experiments or in D_2O (Euriso-top CEA group, 99.9% D) for neutron scattering measurements. The salt-free aqueous solutions of TMAPSS were prepared in both H_2O and D_2O for neutron scattering measurements. All these solutions were heated until complete dissolution (at 50 °C for 1 h) and then let stand for at least 2 days prior to the measurements at room temperature. Concentrations are determined from the masses of solute and solvent by using the tabulated partial molar volumes[56,57] and also by taking into account the water contents of the various PSS powders. Solutions are then characterized by their monomer concentration c (mol/L) and their fraction of NaPSS macromolecules X, as defined by the molar ratio $X = n(\text{NaPSS})/[n(\text{NaPSS}) + n(\text{CaPSS})]$ (because NaPSS and CaPSS samples have identical macroions, n can also be considered as a monomer concentration, in mol/L). Under this procedure, $X = 0$ and 1 correspond to pure CaPSS and NaPSS, respectively.

2.2. Small-Angle X-ray and Neutron Scattering (SAXS and SANS) Measurements. SAXS experiments were carried out in our laboratory with a diffractometer developed by Bruker-Anton Paar (Nanostar). This diffractometer operates with a pinhole collimator and a two-dimensional multiwires proportional detector. A monochromatic ($\lambda = 1.54$ Å with $\Delta\lambda/\lambda = 4\%$) and almost parallel beam (divergence of the order of 0.03°) is obtained through cross-coupled Göbel mirrors. The size of the incident beam on the sample is close to 300 μm. The sample−detector distance was set at 1 m. This configuration allowed us to perform measurements in the q range 0.02 Å^{-1} < q < 0.2 Å^{-1}, with a q resolution related to the beam size on the sample and the beam divergence close to 0.003 Å^{-1}. q is the magnitude of the scattering vector, defined by the wavelength of the incident beam λ and the angle between incident and scattered beam θ such that $q = (4\pi/\lambda)\sin(\theta/2)$. The samples were held in calibrated mica cells of 1 mm thickness, avoiding multiple scattering. Six concentrations were investigated at room temperature for each solute mixture ($X = 0$, 0.25, 0.5, 0.75, 1): $c = 0.0425$, 0.085, 0.17, 0.34, 0.68, and 1.36 mol/L.

SANS experiments were performed at the Institut Laue Langevin (Grenoble, France) on the D11 and D22 diffractometers. Measurements on D11 were done using two different configurations (sample-to-detector distances: 4.10 and 13.50 m) covering a total q range 0.005 < q < 0.12 Å^{-1} at $\lambda = 4.51$ Å ($\Delta\lambda/\lambda = 10\%$). To the subsequent 10% in $\Delta q/q$ have to be added the q resolutions related to the beam size on the sample and the beam divergence, which are 0.003 and 0.001 Å^{-1}, at

the respective sample−detector distances. A circular diaphragm of 10 mm in diameter imposed the size of the incident beam on the sample. The scattered intensity was recorded with a 2-dimensional ^{3}He gas detector. Polyelectrolytes solutions were held in a circular quartz container with a thickness of 4 mm. The temperature was kept fixed during the whole experiment (T = 22 °C). Only three concentrations were investigated by using D11: c = 0.0053 mol/L (X = 0 and 1), c = 0.0106 mol/L (X = 0, 0.25, 0.5, 0.75, and 1), and c = 0.0212 mol/L (X = 0, 0.25, 0.5, 0.75, and 1). Measurements on D22 were done using two different configurations (sample-to-detector distances: 1.35 and 14.40 m) covering a total q range $0.0025 < q < 0.5$ Å^{-1} at $\lambda = 8$ Å ($\Delta\lambda/\lambda = 10\%$). Sample thickness was fixed to 1 mm. The other characteristics were close to the previous ones (D11). Two kinds of solutions were then investigated: TMAPSS solutions in H_2O and TMAPSS solutions in D_2O. In this way, monomer (PSS) and counterion (TMA) partial scattering functions were measured. For each kind of TMAPSS solution, two concentrations were considered: c = 0.0425 and 0.34 mol/L.

The scattering data were treated according to the usual procedures for isotropic small-angle scattering.[58] After radial averaging, the spectra were corrected for electronic noise of the detector, empty cell, absorption, and sample thickness. The normalization to the unit incident flux and the corrections of geometrical factors and detector cells efficiency, for the SANS data, were performed using the scattering of H_2O. In the SAXS experiments, the detector response was measured with the help of a ^{55}Fe source. The data were set in absolute scale (with accuracy better than 10%) by using H_2O as standard. In this way, the differential cross section per unit volume $\Sigma(q)$ (cm^{-1}) was obtained for each solution. It is the sum of two terms:

$$\Sigma(q) = \Sigma^{coh}(q) + \Sigma^{B}(q) \quad (1)$$

$\Sigma^{coh}(q)$ is the coherent differential cross section containing all the information needed to describe the structure of the solution; $\Sigma^{B}(q)$ is the background which has to be removed from $\Sigma(q)$ in order to obtain $\Sigma^{coh}(q)$.

For X-ray scattering, $\Sigma^{B}(q)$ is due to the scattering of the solvent. It is subtracted by using the differential cross section measured from the solvent alone $\Sigma^{S}(q)$ and by taking into account the volume fraction of the solvent in the solution Φ^{S}; i.e., we have

$$\Sigma^{B}(q) = \Phi^{S}\Sigma^{S}(q) \quad (2)$$

Such an approach is only approximate since the scattering related to density fluctuations of free counterions is neglected. However, it is a rather good approximation since $\Sigma^{coh}(q)$ is large compared to $\Sigma^{B}(q)$ in the q range explored here, which is mainly concerned with the position of the maxima of the scattering functions.

For neutron scattering measurements, $\Sigma^{B}(q)$ also involves the incoherent scattering of the solute (macroion plus counterions) that can be written as $cN\sigma^{inc}/4\pi$ in which c is the monomer concentration (mol cm^{-3}), σ^{inc} the monomer incoherent cross section (cm^2), and N Avogadro's number (mol^{-1}). Neglecting inelastic effects, since the wavelengths of the used incident beams are rather low, σ^{inc} can be computed from the values listed in the literature.[59] The background is then described by eq 3.

$$\Sigma^{B}(q) = \Phi^{S}\Sigma^{S}(q) + cN\sigma^{inc}/4\pi \quad (3)$$

At this stage, to make more meaningful the comparisons between several solutions of the same polymer, we consider the ratios of the coherent differential cross sections to the concentration $\Sigma^{coh}(q)/c$ (cm^2/mol).

Since we have a multicomponent solute made of large macroions and small counterions, $\Sigma^{coh}(q)$ actually involves three partial scattering functions:

$$\Sigma^{coh}(q) = K_m^{\,2}S_{mm}(q) + K_c^{\,2}S_{cc}(q) + 2K_mK_cS_{mc}(q) \quad (4)$$

In this relation m refers to macroions and c to counterions; K_m and K_c are the related contrast lengths. As Na−CaPSS aqueous solutions are studied by neutron scattering, counterions can be neglected. The signal is then proportional to the macroion partial scattering function. For TMAPSS solutions in H_2O, it is the same since the scattering length density of TMA (-0.64×10^{10} cm^{-2}) is quite close to that of H_2O (-0.56×10^{10} cm^{-2}). Contrarily, for TMAPSS solutions in D_2O, the signal is proportional to the counterion partial scattering function since the scattering length density of PSS_d (6.39×10^{10} cm^{-2}) matches the one of D_2O (6.38×10^{10} cm^{-2}). Now, as Na−CaPSS aqueous solutions are studied by X-ray scattering, the signal is no longer reduced to any partial scattering function, and we are bound to consider the three terms of eq 4.

2.3. Remarks on Other Scattering Measurements from the Literature. Besides our scattering results on mixed valence systems, we will also recall in this paper various SAXS and SANS results reported in the literature in the case of monovalent counterions only.[60−64] They are related to salt-free solutions in good solvents of different dielectric constants and to linear flexible polyelectrolytes of distinct charge fractions, above and below the counterion condensation threshold. For all these polyelectrolyte solutions, we have considered the position in the reciprocal space, q^*, of their scattering peak and studied its change as the concentration (in mol/L) is varied. The conversion from g/L (often used in the selected papers) to mol/L requires a precise knowledge of the mean molar masses of the monomers, which depends on the charge fraction f and the water content τ_w of the initial dried samples. Unfortunately, these characteristics are not stated in all papers; therefore, a small uncertainty remains in the determination of the monomer concentration in mol/L. A brief description of the main features of the related systems is given in Table 2. For some figures, we also consider additional light scattering results obtained from NaPSS salt-free aqueous solutions[65] by Drifford et al.

2.4. Static Fluorescence. Pyrene with an excitation wavelength of 335 nm was used as fluorescent probe. Fluorescence spectra of pyrene molecules dissolved in NaPSS or CaPSS aqueous solutions were recorded on a Hitachi F-4010 spectrofluorometer between 350 and 500 nm. They allow to test the existence of possible hydrophobic microdomains. Indeed, the vibronic fluorescence spectra of pyrene exhibit five peaks (denoted 1 to 5), and the ratio I_1/I_3 of the intensities of the first and third peaks depends on the polarity of the environment of the pyrene molecules. It is close to 1.8−1.9 in water, at room temperature, and reaches 0.9 in nonpolar solvents. This ratio was measured as a function of the polyelectrolyte concentration.

3. Results

3.1. Scattering Profiles at Low Concentrations (c < 0.1 mol/L). Typical SANS and SAXS measurements at two distinct concentrations in the semidilute regime (c = 0.0212 and 0.0425 mol/L) are presented in Figure 1.

The scattering profiles exhibit a clear broad maximum as encountered with salt-free aqueous solutions of NaPSS or CaPSS in former works.[66,60−69] We call q^* the abscissa of this peak. One stringent feature is the q^* variation with X, i.e., the counterion valence. On one hand, q^* is nearly constant for X = 0.5, 0.75, and 1. These three mixtures show almost identical scattering profiles and therefore should exhibit very similar structures. On the other hand, for X = 0.25 and 0, q^* is shifted to lower q values while the intensity of the peak increases. Since the PSS macroions are identical for all the samples, the origin of these modifications has to be related to changes in the valence of the counterions.

As previously mentioned, the scattered intensity is mainly related to macroions for neutron scattering while

Table 2. Characteristics of the Samples Used To Validate the Scaling Theory and the Manning−Oosawa Approach of the Counterion Condensation for Polyelectrolyte Solutions in the Presence of Monovalent Counterions[a]

sample	solvent	ϵ	l_B	f	ζ	ref
NaPSS ($X = 1$)	H_2O	78	7.14	0.90	2.51	this work
NaPSS* ($X = 1$)	$(H_2O)_{0.75} + THF_{0.25}$	60	9.22	0.90	3.21	this work
TMAPSS	H_2O or D_2O	78	7.14	1	2.79	this work
NaPSS	H_2O	78	7.14	1	2.79	65
AMANPS (95%)	H_2O	78	7.14	0.95	2.65	63
AMANPS (60%)	H_2O	78	7.14	0.60	1.67	63
AMANPS (51%)	H_2O	78	7.14	0.51	1.42	63
MPCP	DMF	36.7	15.3	1	5.98	64
MPCP	PC	64.9	8.6	1	3.36	64
PMVP	EG_D	37.7	14.9	0.45	2.62	62
PMVP	D_2O	78	7.14	0.45	1.25	62
NaAD10	H_2O	78	7.14	0.015	0.04	60
NaAD17	H_2O	78	7.14	0.07	0.19	60
NaAD27	H_2O	78	7.14	0.17	0.47	60
NaAD37	H_2O	78	7.14	0.27	0.75	60
NaAD60	H_2O	78	7.14	0.35	0.98	60
NaPVS ($\alpha = 5.4\%$)	H_2O	78	7.14	0.054	0.15	61
NaPVS ($\alpha = 10.7\%$)	H_2O	78	7.14	0.107	0.30	61
NaPVS ($\alpha = 23.2\%$)	H_2O	78	7.14	0.232	0.65	61
NaPVS ($\alpha = 31\%$)	H_2O	78	7.14	0.31	0.86	61
NaPVS ($\alpha = 49.9\%$)	H_2O	78	7.14	0.499	1.39	61

[a] The monomer size b is 2.56 Å for all the samples; f is the fraction of charged monomers, or the charge fraction; the mean distance between charges along the chemical sequence of the macroions is $A = b/f$; ϵ is the dielectric constant; l_B is the Bjerrum length (Å) for the solvent considered, at $T = 25$ °C; $\zeta = l_B/A$ is the Manning charge parameter. AMAMPS are samples of poly[acrylamide-*co*-sodium-2-acrylamido-2-methylpropanesulfonate]; MPCP, a sample of atactic poly[2-(methacryloyloxy)ethyltrimethylammonium 1,1,2,3,3-pentacyanopropenide]; PMVP, a sample of poly[*N*-methyl-2-vinylpyridinium chloride]; NaAD series, sodium salts of acrylamide−acrylic acid copolymers of distinct compositions; NaPVS, sodium salts of partially sulfuric acid esterificated poly(vinyl alcohol). The solvent DMF is *N*,*N*-dimethylformamide; EG, ethylene glycol; PC, 1,2-propylene carbonate. NaPSS* has been dissolved in a solvent which is a mixture of H_2O and THF (tetrahydrofuran) with volume fractions of 75 and 25%, respectively. The corresponding dielectric constant has been evaluated from those of its components, $\epsilon(H_2O)$ and ϵ(THF), using the relationship $\epsilon = 0.75\epsilon(H_2O) + 0.25\epsilon$(THF).

it is due to both counterions and macroions for X-ray scattering. So, the peak intensity for X-ray scattering is very sensitive to the fraction as well as the nature of condensed counterions.

3.2. Scattering Profiles at Higher Concentrations (c > 0.1 mol/L). As the concentration is increased, new features are observed (Figure 2). The scattering curves are now all different for all mixtures. Both the position q^* and the intensity $I(q^*)$ of the scattering peak are affected: q^* is shifted to lower q values, and $I(q^*)$ increases when X is varied from 1 to 0.

The structure of the aqueous solutions is now strongly dependent on X. Upon further increase in concentration, the scattering peak gradually disappears, provided Ca counterions are present, i.e., for $X < 1$. This effect is more and more pronounced when X decreases. That point is illustrated in Figure 3 for $X = 0$, i.e., for CaPSS solutions. The scattering peak vanishes above $c = 0.68$ mol/L. The scattering curves then look very similar to those of neutral polymers. For $X = 0.5$, the peak disappears only around $c = 1.36$ mol/L: the peak melting concentration is shifted to larger c values.

3.3. Variations of q^* with Respect to c. The variations of q^* with respect to c for distinct X values are shown in Figure 4. The main features are the following:

(i) For the lowest concentrations (inset in Figure 4), q^* scales as $c^{1/2}$ within experimental uncertainties for all the solutions. This behavior is in accordance with scaling predictions for polyelectrolytes in good solvent conditions; it has already been observed for pure NaPSS.[65−69] It must be noted that other measurements (data not shown), performed on NaPSS with a still higher degree of sulfonation ($\tau_s = 1$), give quite identical results (equal q^* values). Thus, we will neglect the effect of a nonperfect sulfonation in our discussion of the data and will consider our PSS samples as fully sulfonated ones.

(ii) For these lowest concentrations, the prefactor of the $c^{1/2}$ scaling law is almost identical for $X = 1$, 0.75, and 0.5 (a careful inspection for $X = 0.5$ however denotes a small decrease) whereas a large discrepancy is observed for $X = 0.25$, for which the prefactor is lowered, and for $X = 0$, for which it is even lower.

(iii) For higher concentrations (c > 0.1 mol/L), deviations from the $c^{1/2}$ scaling law are observed for all mixtures containing Ca counterions. This trend is more pronounced as the fraction of Ca counterions is increased; the scaling exponent being reduced from 0.5 (the exact value being less than 0.5 as discussed later) to 0.2 as X varies from 1 (100% Na) to 0 (100% Ca).

(iv) For the highest concentrations and $X = 0$, 0.25, and 0.5, the peak disappears. The critical melting peak concentration is highly sensitive to the presence of divalent counterions and is displaced to lower c values when X is decreased.

To summarize sections 3.1−3.3, all observations strongly suggest an important role of the counterion valence on the structure of the polyelectrolyte solutions. However, at low concentration, it is striking to see how valence effects are absent or masked (we will see why below) for the higher X values (1, 0.75, and 0.5).

4. Theoretical Background: Condensation and Scaling

Let us now recall the accepted picture for linear polyelectrolytes in the presence of monovalent and or divalent counterions, at two levels: first, the counterion condensation process; second, the scaling description of macroions and, more especially, that of the characteristic scattering peak of their semidilute solutions. In a third part, we will show how the combination of counterion condensation and scaling improve data agreement with the scaling model, in the case of monovalent counterions.

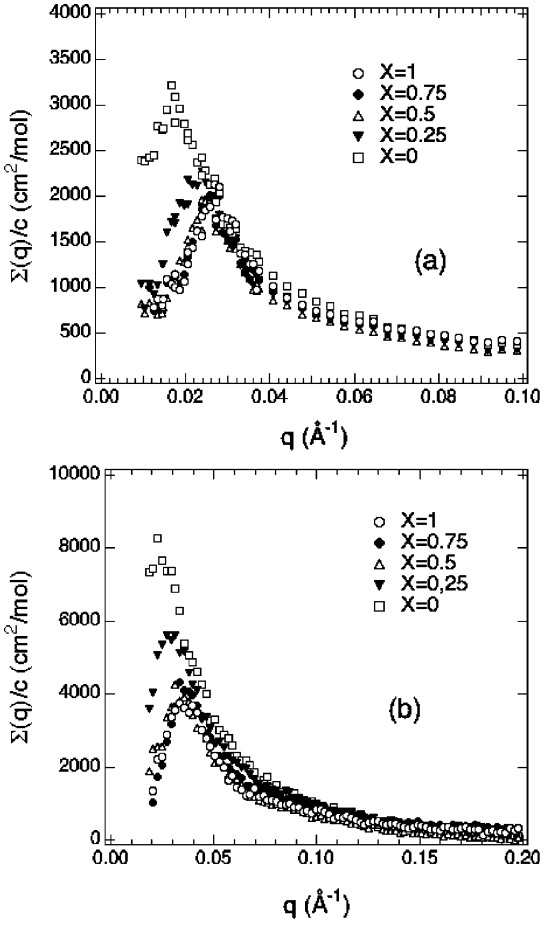

Figure 1. Scattering from salt-free aqueous solutions of mixed NaPSS and CaPSS polyelectrolytes. (a) SANS profiles recorded at $c = 0.0212$ mol/L for different fractions of NaPSS polyelectrolytes ($X = 0$, 0.25, 0.5, 0.75, and 1). (b) SAXS profiles recorded at $c = 0.0425$ mol/L for different fractions of NaPSS polyelectrolytes ($X = 0$, 0.25, 0.5, 0.75, and 1).

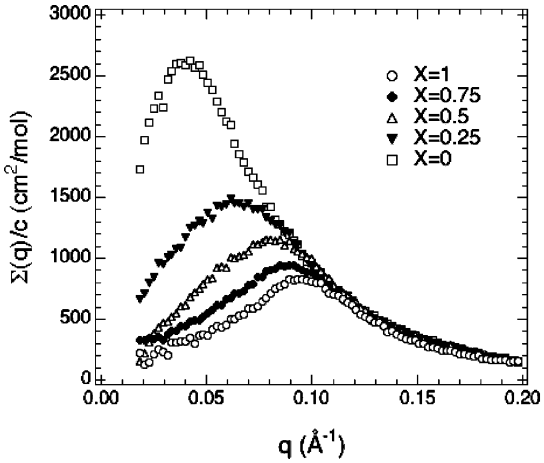

Figure 2. SAXS profiles of salt-free aqueous solutions of mixed NaPSS and CaPSS polyelectrolytes, recorded at $c = 0.34$ mol/L for different fractions of NaPSS polyelectrolytes ($X = 0$, 0.25, 0.5, 0.75, and 1).

4.1. Counterion Condensation: The One and Mixed Valence Cases. We have investigated different mixtures of NaPSS and CaPSS. The relevant parameter is the fraction of NaPSS chains, X, that varies from 0 (pure CaPSS) to 1 (pure NaPSS). Since fully sulfonated polystyrene is a highly charged macroion, a counterion condensation process is expected to take place from most

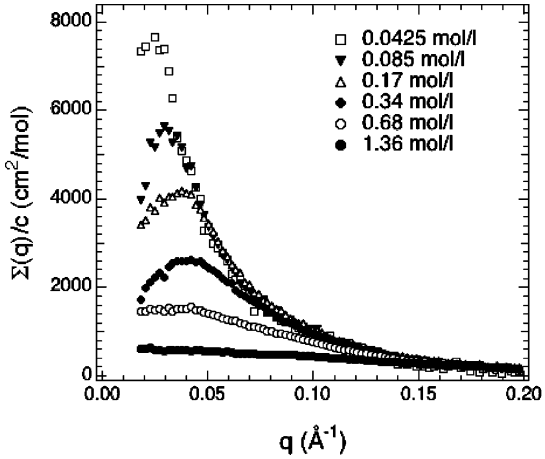

Figure 3. SAXS profiles of salt-free aqueous solutions of pure CaPSS polyelectrolytes ($X = 0$), recorded at different monomer concentrations.

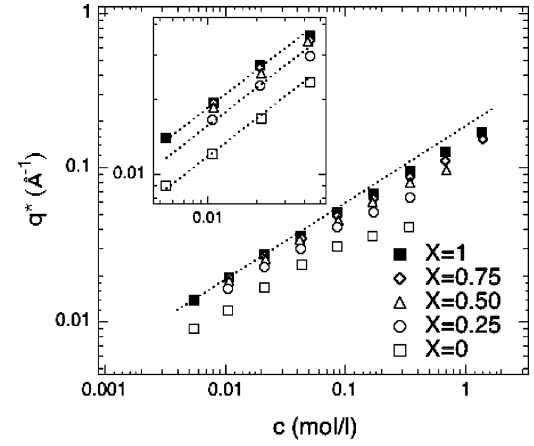

Figure 4. Scattering vector q^* vs monomer concentration c for different fractions of NaPSS polyelectrolytes ($X = 0$, 0.25, 0.5, 0.75, and 1). For $X = 0$ and 0.25, the maximum of the scattering function is no longer really observable as $c > 0.34$ mol/L. The insert is concerned with the results obtained for the lowest concentrations ($c < 0.05$ mol/L). Dotted lines correspond to a $c^{1/2}$ evolution.

experimental and theoretical points of view.[40,41,53,63] It is therefore necessary to examine this process for any X value.

For identical counterions of valence Z, according to Manning, a condensation process takes place when the charge parameter $\zeta = l_B/A$ is larger than $1/Z$.[40] As defined in Table 2, l_B is the Bjerrum length and A is the mean distance between charges along the chemical sequence of the macroions. The linear charge density is then renormalized to a constant value such that $A = Zl_B$ or $\zeta = 1/Z$. The condition $\zeta > 1/Z$ or $l_B/A > 1/Z$, that is also the strong-coupling limit, corresponds to $A < l_B$ for monovalent counterions and $A < 2l_B$ for divalent counterions. Such conditions are always fulfilled with our systems, and thus there is always a charge renormalization tending to reduce ζ to the net value $1/Z$. The charge fraction f (equals to 1 in the absence of any counterion condensation, i.e., one electrostatic charge every monomer of size b) is therefore decreased to the effective value $f_{eff} = b/Zl_B$. There should be one effective charge every l_B for pure NaPSS ($X = 1$) and one effective charge every $2l_B$ for pure CaPSS ($X = 0$). Hence, we can view counterions as distributed in two populations: condensed counterions which are confined in small volumes around the macroions by the macroion poten-

tial well (which let them some mobility along the macroions) and free counterions which escape the macroion potential well and scatter in the solution.[41]

For mixtures of monovalent (Na) and divalent (Ca) counterions, the condensation process is more complex.[44,70] Counterions with the higher valence will condense first and the Manning charge parameter will be reduced to ζ' according to the amount of condensed counterions:

(i) If there are enough divalent counterions to reduce ζ to $\zeta' = 1/2$, then the condensation process stops and the excess of Na and Ca counterions remains free in the solution. Among the set of solutions investigated here, this is only the case for the ones corresponding to $X = 0$ (pure CaPSS). The effective charge fraction is therefore $f_{\text{eff}} = b/2l_B$ (0.18 in our particular case).

(ii) For solutions of larger X values ($X = 0.25$, 0.5, 0.75), different regimes may appear. If there are not enough divalent counterions to achieve $\zeta' = 1/2$ but enough to make $1/2 < \zeta' < 1$, all Ca counterions will be condensed whereas all Na counterions will remain free in the solution. That is the case for $X = 0.25$. In that mixture, the condensation of all the Ca counterions leads to one effective charge every four monomers (approximately one effective charge every 10 Å along the PSS chemical sequence). Here, we are within an interesting regime where one can gradually change the effective charge, with only Ca species condensed on the macroion. Actually, the effective charge fraction becomes equal to X.

(iii) Finally, if after condensation of the Ca counterions ζ' is still larger than 1, then Na counterions will also condense to reduce ζ' to $\zeta'' = 1$ (one electrostatic charge every $l_B = 7.14$ Å in water). Part of Na counterions will be condensed; the other part will be free. This is expected for $X = 0.5$, 0.75, and 1. This is another surprising regime: although the ratio of monovalent to divalent condensed counterions is changed according to X, the effective charge fraction ($f_{\text{eff}} = b/l_B$, i.e., close to 0.36) and the amount of free counterions (all monovalent) are constant.

To sum up, the expected variation of the effective charge fraction f_{eff} as a function of X is shown in Figure 5a. Moreover, a schematic picture is proposed in Figure 5b.

We see now the interest of the mixed valence systems: they should allow us to gradually change the mean distance between effective charges along the chemical sequence of the macroions (within a certain X range) and the proportion of Na and Ca counterions in the condensed and free counterion populations. In this way, the role of the effective charge fraction as well as the nature of condensed and free counterions on the structure of the solutions can be probed.

This Manning−Oosawa description is strictly valid only for an infinite dilution together with a rodlike conformation of the macroions. However, it is in accordance with experiments performed on flexible polyelectrolytes in a finite concentration range.[53,61,63,71,72] Thus, we will consider it as a reasonable approximation.

4.2. Scaling Description of Charged Linear Polymers. In the dilute regime ($c < c^*$), the average conformation of the macroions is highly stretched due to electrostatic interactions. On the other hand, the scattering experiments reveal the existence of a peak at a position q^* that scales as $c^{1/3}$. This peak can be interpreted as the signature of a position order, i.e., a

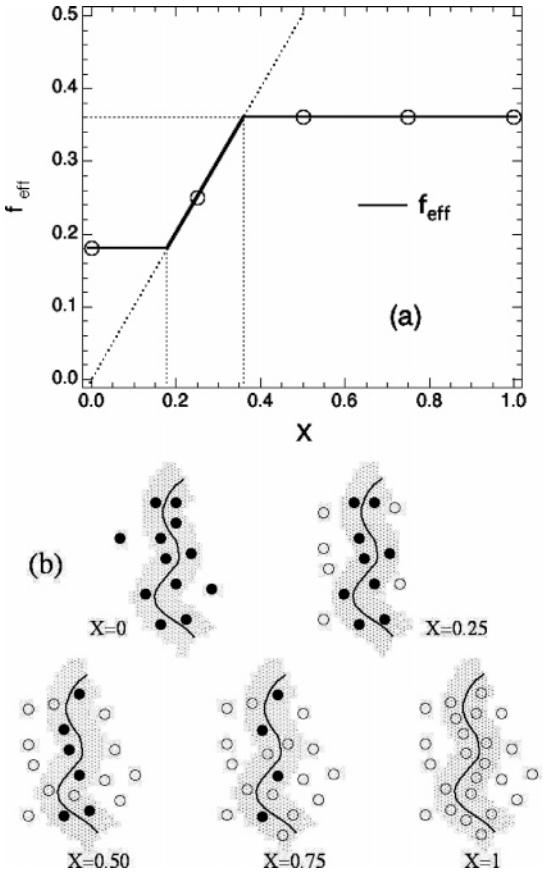

Figure 5. Main characteristics of Na−CaPSS mixtures, according to the Manning−Oosawa approach. (a) Effective charge fraction f_{eff} vs fraction of NaPSS polyelectrolytes X. Open circles correspond to experimental X values of the present work. (b) Schematic representation of condensed and free counterions for different fractions of NaPSS polyelectrolytes ($X = 0$, 0.25, 0.5, 0.75, and 1). Open and filled circles correspond to Na and Ca counterions, respectively. Condensed counterions are located in the shadow area around the macroion. Note that the number of Na and Ca counterions is only indicative. In this schematic representation, the macroion contains 24 charged monomers. $X = 1$; the free and condensed counterions are Na counterions; $X = 0.75$, 0.5, and 0.25; the free counterions are Na counterions; $X = 0.75$ and 0.5; the condensed counterions are mixtures of Na and Ca counterions; $X = 0.25$ and 0; the condensed counterions are Ca counterions; $X = 0$; the free and condensed counterions are Ca counterions.

preferred average distance between the centers of mass of the macroions. In the semidilute regime ($c > c^*$), the macroions interpenetrate each other. A single broad scattering peak is still present but it scales now as $c^{1/2}$.

The structure of the semidilute solutions has been analyzed in terms of an isotropic net of rods by de Gennes.[48] The mesh size of this net, ξ, is the only characteristic length. Specifically, it is the screening length of the electrostatic interactions. Thus, for distances smaller than ξ, the electrostatic interactions are dominant, and the average conformation of the macroions remains highly stretched. For distances larger than ξ, the electrostatic interactions are screened, and hence the average conformation of the macroions is a random walk of correlation blobs of size ξ. A scaling argument, similar to that made for neutral polymers in a good solvent, allows to demonstrate that ξ scales as $c^{-1/2}$.[48,49] From an experimental point of view, insight into the structure of the semidilute solutions will be gained through the position of the single broad scattering maximum that scales as ξ^{-1}. Such a maximum is indeed

associated with an electrostatic correlation hole, each part of a given macroion being surrounded by an excluded volume of size ξ from which other macroions are partly expelled.[67,73]

The scaling approach of de Gennes has been reviewed by Dobrynin, Colby, and Rubinstein.[50] The main new feature is the introduction of a parameter that takes the solvent quality into account. It is also emphasized that the Debye screening length (due to free counterions alone), κ_D^{-1}, could not correctly describe the electrostatic screening in semidilute solutions since κ_D^{-1} is shorter than the average distance between macroions, ξ. In a good solvent condition, the correlation or screening length ξ can be written as

$$\xi = f^{-2/7}(l_B/b)^{-1/7}(bc)^{-1/2} \quad (5)$$

Here, f is the charge fraction of the polyelectrolytes.

A network of interpenetrated rods can crudely schematize this scaling model. The c dependence is then related to the average distance between rods; meanwhile, the f dependence is introduced by considering that the rods are alignments of electrostatic blobs, which defines the mass per unit length of these rods. The electrostatic blob size scales as $f^{-6/7}$ and $f^{-2/3}$ for good and Θ solvent, respectively.

So, the scaling model mainly applies to weakly charged polyelectrolytes for which the charge fraction is the chemical charge fraction of the macroions. However, it is usually assumed also to apply to highly charged polyelectrolytes. In the weak-coupling limit ($\zeta < 1/Z$), eq 5 remains valid. In the strong-coupling limit ($\zeta > 1/Z$), the macroions are then treated as weakly charged polyelectrolytes with an effective charge fraction f_{eff} taking into account the condensation of part of the counterions. In this case, we propose to replace relation 5 by

$$\xi = f_{eff}^{-2/7}(l_B/b)^{-1/7}(bc)^{-1/2} \quad (5')$$

Obviously, for the mixed valence systems (Na−CaPSS), ξ therefore depends on X. Equations 5 and 5′ mostly show that the screening length ξ and therefore the position of the broad scattering peak q^* depend on the charge fraction of the macroions (or their effective charge fraction when a condensation of part of the counterions takes place) and concentration. But they also depend on the dimensionless parameter l_B/b.

4.3. Scaling and Condensation: Comparison with Experiments Involving Monovalent Counterions. In this section we focus on the case of monovalent counterions in order to test the validity of the scaling approach combined with condensation.

4.3.1. Master Curve. We will consider various flexible macroions in good solvent and will compare the q^* values measured by us or extracted from the literature with the theoretical expression 5 for $2\pi/\xi$, using the sample characteristics of Table 2. More precisely, ξ is calculated from eq 5 in the weak-coupling limit ($\zeta < 1/Z$), while it is rather obtained from eq 5′ in the strong-coupling limit ($\zeta > 1/Z$). Since only monovalent counterions are considered, $f_{eff} = b/l_B$, and eq 5′ can be written as

$$\xi = (l_B/b)^{1/7}(bc)^{-1/2} \quad (5'')$$

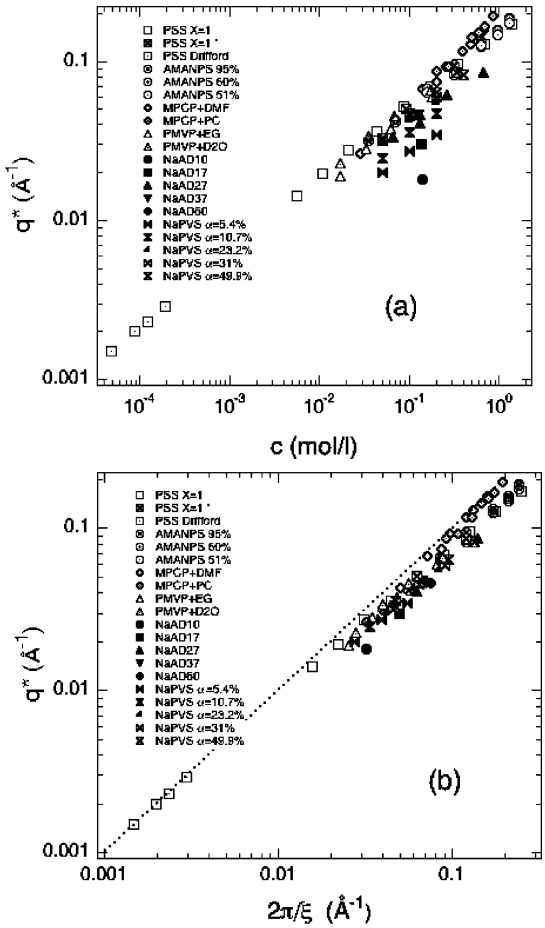

Figure 6. Scattering vector q^* vs c and $2\pi/\xi$ for various flexible polyelectrolytes in the presence of monovalent counterions. (a) q^* vs c; (b) q^* vs $2\pi/\xi$. The counterion condensation phenomenon has been taken into account according to the Manning−Oosawa approach. Dotted line indicates the strict equality $q^* = 2\pi/\xi$.

In this way, we take into account the counterion condensation through the Manning−Oosawa theory.

If ξ correctly describes the systems, plotting q^* as a function of $2\pi/\xi$ instead of simply the concentration should lead to a master curve. The q^* values for all the polyelectrolytes listed in Table 2 are presented as a function of c in Figure 6a. The same data are reported as a function of $2\pi/\xi$ in Figure 6b.

A master curve, linking q^* and $2\pi/\xi$, is clearly obtained over more than 4 decades in concentration, provided the counterion condensation process is taken into account. The scaling model is therefore able to explain small modifications when changing from one solvent to another as well as variations with the charge density, when combined with condensation.

If the condensation of counterions is not accounted for, neither the nearly constant values of q^* encountered in AMANPS (for different charge fractions) nor the appearance of a plateau in NaPVS for the highest values of the dissociation degree (α) can be explained. Moreover, nor can the q^* values for PMVP samples in different solvents (EG, D_2O) or MPCP in DMF and PC be correctly rescaled.

Looking more in detail, we can point out a small dispersion in the data forming the master curve in Figure 6b. This is undoubtedly related to uncertainties in scattering measurements as well as in the characteristics of the polyelectrolyte solutions necessary to

evaluate ξ (Table 2). Furthermore, as will be seen in the next subsection, scattering length density of both counterion and macroion may also play a relevant role in the data dispersion.

In this approach, we decided not to use the Debye length as the typical length scale of the system. For NaPSS solutions, the Debye length κ_D^{-1} (using $\kappa_D^2 = 4\pi l_B I$ and the ionic strength $I = \sum_i Z_i^2 c_i$) caused by the free counterions is always smaller than the average distance between chains (extracted from the relation $d = 2\pi/q^*$). This remains correct if the condensation is no longer taken into account. For instance, κ_D^{-1} is close to 35 Å at $c = 0.0425$ mol/L (and 9 Å at $c = 0.68$ mol/L), whereas the average distance between chains is close to 175 Å (50 Å at 0.68 mol/L). Thus, the use of κ_D^{-1} as the screening length is not appropriate without added salt since electrostatic interactions occur at distances well above the Debye length. Furthermore, the Debye length is even smaller than the average distance between counterions (with or without taking the condensation into account). However, the fact that κ_D and ξ^{-1} scale as $c^{1/2}$ demonstrate that both quantities are proportional to each other. Thus, rescaling q^* as a function of κ_D instead of ξ^{-1} should lead to similar results. In fact, this is not the case. For monovalent counterions, κ_D is equal to $(4\pi l_B f)^{1/2} c^{1/2}$ (without condensation) or $(4\pi b)^{1/2} c^{1/2}$ (with condensation). Thus, modifications of the solvent (l_B) or the charge fraction f do not change κ_D and ξ^{-1} a similar way. It is known from an experimental point of view that q^* scales as $f^{1/3}$ (or $f^{2/7}$). Such a result is not compatible with the Debye length description.

4.3.2. Deviations at Higher Concentrations. A more systematic effect is however visible from closer inspection: the strict equality $q^* = 2\pi/\xi$ is perfectly obeyed only in a lower c range. Deviations toward lower q^* values are observed beyond a certain c (or q^*) value. They correspond to deviations from the usual $c^{1/2}$ scaling law, which gradually increase with c. A first cause could be a progressive increase in the counterion condensation, leading to a continuous decrease in the effective charge fraction.[20,74] In Appendix A, we rule this out because it leads to unrealistic changes in the effective charge fraction and/or the counterion condensation threshold. We can notice that the observed deviations depend on the explored q range. They are negligible at low spatial resolution (low q), i.e., in light scattering experiments, and increase at high q, as the resolution is improved. They also depend on the contrast and/or the kind of radiation used for the experiments. For example, with NaPSS salt-free aqueous solutions, such deviations are observed by SAXS whereas they are almost unobservable by SANS when D_2O is used as solvent. This dependence on the contrast can be definitely demonstrated by comparing SANS results obtained with solutions of TMAPSS in H_2O and D_2O, at the same concentration. This comparison, which turns out to compare the macroion and counterion partial scattering functions ($S_{mm}(q)$ and $S_{cc}(q)$, respectively), is made in Figure 7.

Obviously, the q^* of $S_{cc}(q)$ is lower than the one of $S_{mm}(q)$. This is consistent with computer simulations performed on salt-free solutions of rigid polyelectrolytes.[82] This shift also depends on concentration: it is rather weak for low concentrations but increases with c. It is caused by a modification of the form factor rather than the intermolecular term. Indeed, the q^* that should

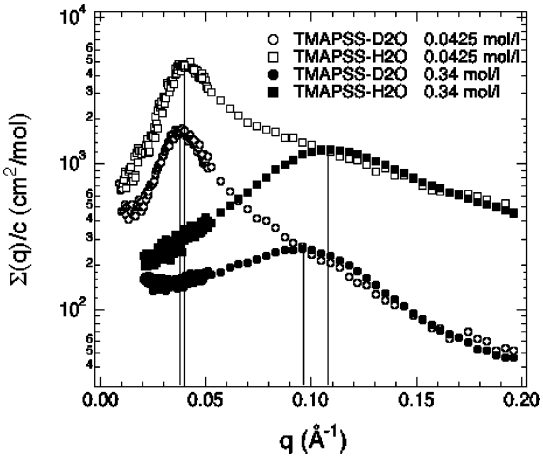

Figure 7. SANS profiles of salt free solutions of TMAPSS in H_2O and D_2O. They are proportional to the macroion and counterion partial scattering functions ($S_{mm}(q)$ and $S_{cc}(q)$, respectively). Two monomer concentrations are considered: $c = 0.0425$ and 0.34 mol/L. For each monomer concentration, the scattering vector q^* of $S_{cc}(q)$ is lower than the one of $S_{mm}(q)$.

be compared to $2\pi/\xi$ is actually the one of the intermolecular scattering function.[75] By measuring the total scattering function, involving the form factor as well as the intermolecular correlations, discrepancies are expected. They are different for $S_{cc}(q)$ and $S_{mm}(q)$ because the form factor of the sheath of the condensed counterions around one macroion differs from that of the macroion itself. A sharper decrease in the sheath form factor shifts the maximum of the total scattering function toward smaller q values. Since this decrease is marked at high q values, it leads to a larger shift as the concentration increases. Remarkably, discrepancies in q^* measurements are negligible as the macroion (PSS) partial scattering functions are considered. On the contrary, when the counterion partial scattering functions are involved, they cannot be neglected. This is especially the case for SAXS experiments. We finally performed SAXS measurements on TMAPSS (data not shown). This counterion also presents remarkable properties toward X-ray scattering since the total scattering function is very close to S_{mm}. In that case the $c^{1/2}$ scaling law is perfectly obeyed. Furthermore, the position of the maximum q^* is identical to the one observed with neutrons in the S_{mm} structure function.

We definitively see the problems in the q^* values determined from the total scattering function. According to the contrast of both counterions and polyions, q^* may vary within a rather large interval (up to 10%). The polyelectrolyte under investigation and the scattering technique also play a role in the data dispersion observed in the previous section.

4.3.3. Size of the Electrostatic Blobs. The use of the scaling approach for highly charged polyelectrolytes assumes that, after counterion condensation, macroions simply behave as if they were partially charged and even weakly charged though the actual charge fraction can still be relatively large (0.36 for NaPSS). This can be questionable. A key point is that the weakly charged polyelectrolyte model lies upon the concept of electrostatic blobs. In practice, even if the counterion condensation is taken into account, electrostatic blobs should be rather small and thus contain only a few monomers (of the order of 3−4 monomers for NaPSS). The derivation of the expression of ξ, in particular the different

exponents associated with f, l_B, and b, lies upon the assumptions about the statistic of the chain inside the electrostatic blobs: e.g., the relation between the size and the number of units is the same as in a self-avoiding chain. This assumption may fail for chains of a few monomer units. Despite this, the existence of a master curve seems to validate the scaling description.

Hence, we reach a first intermediate conclusion: except for the higher concentrations where other scattering effects may come into play, the scaling approach combined with condensation correctly describes the polyelectrolyte peak position in the case of monovalent counterions.

5. Na−CaPSS Mixtures: Interpretive Discussion

We have just seen that Figure 6b evidences the existence of condensation threshold and charge renormalization effects on scattering curves in the case of monovalent counterions. Let us now return to the measurements reported in this paper on mixtures of Na and Ca counterions. Obviously, they open the way of modifying the effective charge fraction without changing the chemical structure of the macroions. We will thus compare our scattering results on these mixtures in the light of the scaling−condensation predictions.

5.1. Qualitative Interpretation. Let us first compare the scattering curves of Na−CaPSS mixtures according to their state of counterion condensation.

In the low concentration regime (c < 0.1 mol/L), our measurements show that q^* is nearly identical for X = 1, 0.75, and 0.5 and decreases for X = 0.25 and 0. According to the scaling−condensation approach, this suggests similar effective charge for the three higher X values and a reduction for the two others. These deductions are in accordance with our description of the counterion condensation process (section 4.1) which predicts the same effective charge fraction for X = 1, 0.75, and 0.5 as well as smaller values for X = 0.25 and 0. Moreover, these deductions are reinforced by the analysis of the height of the scattering peak $I(q^*)$. To make it quantitative, let us recall that the contrast in X-rays is partly due to the condensed counterions or, more precisely, to their electronic density. Exchanging Na for Ca counterions (as expected when changing the X value) is ruled by a particular balance: the electronic charge of Ca (18 e^-) is about twice that of Na (10 e^-), which is similar to the ratio between their ionic charge (2/1); changing one Ca (18 e^-) for two Na counterions (2 × 10 e^-) does not greatly affect the total number of electrons. For X = 1, 0.75, and 0.5, since the effective charge is constant, one condensed Ca counterion has to be replaced by two Na ones. Thus, the number of electrons in the condensed cloud of monovalent and divalent counterions is roughly constant. Because the molar volumes of both counterions are almost identical, their electronic density is constant (their contrast lengths in water are similar). Hence, the fact that the height of the scattering peak does not greatly change is a proof of an identical structure and may validate our condensation description at least for the highest X values.

The scattering features therefore provide a clear signature of a charge renormalization. A simple description of the condensation process associated with the scaling approach enables a qualitative interpretation of the scattering curves. However, as will be shown in the next sections, the effective charge fraction is not the only parameter that can be involved for CaPSS (X = 0) aqueous solutions, even in the low concentration regime.

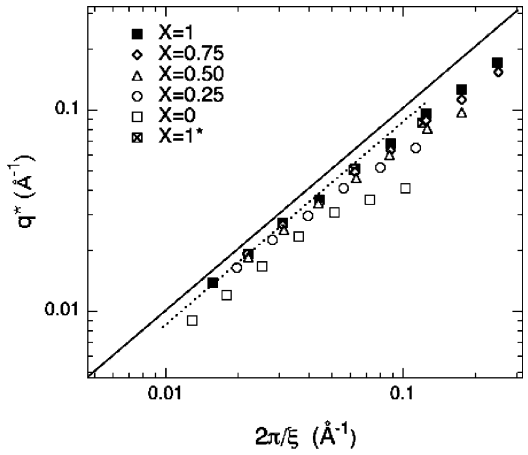

Figure 8. Scattering vector q^* vs $2\pi/\xi$ for different fractions of NaPSS polyelectrolytes (X = 0, 0.25, 0.5, 0.75, and 1). The line corresponds to the strict equality $q^* = 2\pi/\xi$. The dotted line corresponds to $q^* = \alpha/\xi$ with $\alpha < 2\pi$.

At higher concentrations (c > 0.1 mol/L), there are new features: q^* is now different for each X value, which is not compatible with our description, and is followed by a modification in the scaling exponent that is more pronounced when the proportion of Ca counterions is increased. We recall that all divalent counterions are supposed to be condensed for X = 0.25, 0.5, and 0.75 mixtures.

In summary, for the higher c regime (c > 0.1 mol/L) and contrarily to the lower c regime, the nature of the condensed counterions plays a role that cannot be only explained by a charge renormalization as predicted by the Manning−Oosawa theory. Pure NaPSS is not really affected, at least within the investigated c range, although the counterion condensation is expected to be slightly and continuously improved as the concentration is increased.[20] The important influence of counterion valence on the structure of polyelectrolyte solutions is therefore revealed. We will pursue this discussion in section 5.4.

5.2. Comparison with Scaling Predictions. In section 4.3, we have shown that the correlation length ξ developed in the scaling model is able to correctly describe the evolution of q^* for different flexible polyelectrolyte solutions, at least in the case of monovalent counterions. We can now test this approach for polyelectrolytes in the presence of mixed valence counterions (specifically, mixtures of monovalent and divalent counterions). The presence of divalent counterions will be taken into account through the effective charge fraction, f_{eff}, which we introduce in the scaling model.

The evolutions of q^* for distinct X values are presented in Figure 8 as a function of $2\pi/\xi$, calculated according to eq 5′.

Figure 8 shows that the scaling model accounts rather well for SAXS measurements in the low concentration regime, except for pure CaPSS (X = 0). In a first approximation, these observations may validate the Manning−Oosawa description of the counterion condensation process for mixtures of monovalent and divalent counterions, except for X = 0.

For pure CaPSS, i.e., X = 0, it is obvious that another phenomenon is present which is not properly taken into account by the scaling approach. We can therefore argue

that, except for pure CaPSS, the valence of the condensed counterions has practically no effect on the structure of the solutions other than the one related to a charge renormalization, in agreement with the Manning−Oosawa theory.

Hence, we reach a second intermediate conclusion: in the low concentration regime, the scaling−condensation model correctly describes the polyelectrolyte peak position for a mixture of monovalent and divalent counterions except in the range of high Ca fractions (X close to zero).

5.3. Distinctive Features of the Large Ca Fractions ($X \leq 0.25$) in the Low Concentration Regime. The discrepancy for pure CaPSS ($X = 0$) may have a different origin.

5.3.1. Main Scattering Results for $X = 0$. Neutron scattering experiments on pure NaPSS and pure CaPSS aqueous solutions have been already performed.[16,17] They show that q^* is shifted to lower q values for CaPSS in accordance with our measurements. The average size of the macroions was also found to be smaller in the presence of divalent counterions compared to monovalent counterions. These results, which have been confirmed by simulations,[25] were interpreted by Zhang et al.[16] as a consequence of a charge renormalization, namely a reduction in the effective charge fraction similar to the one encountered when the degree of sulfonation of the PSS macroions is decreased, i.e., when the macroion becomes more hydrophobic.[52,53,63,71,76] Conversely, Dubois et al. argued that they were due to a conformational change resulting from bridging-type intramolecular correlations between monomer units through divalent counterions, without implying any hydrophobic character.

In the frame of the scaling approach, the charge fraction or the effective charge fraction determines the size of the electrostatic blobs. Any modification of that parameter may change the size of the extended chains in dilute solution and also the value of the overlap concentration c^*. This is responsible for a shift of the position of the maximum q^* values (as shown from relations 5 and 5′) as well as changes in the radius of gyration. If the counterion condensation process (and, therefore, the effective charge of the macroion) certainly plays an important role as mentioned by Zhang et al., it is thus not necessary to invoke any hydrophobic property to describe the q^* behavior. Nevertheless, this effect is not large enough in the scaling model to correctly explain the experimental observations. We will return to this discussion below; before we would like to stress the main difference between $X = 0$ (pure CaPSS), where the discrepancy is pronounced, and $X = 0.25$, where it is marginal. For $X = 0.25$, which is very close to 0.18, the nature of the free counterions is different. Pure CaPSS is the only one among our systems for which some divalent counterions are free in the aqueous solutions.

Here, we reach a third intermediate conclusion: it is mostly when some divalent counterions are free in the solution that we observe disagreement with the scaling−condensation model.

The scaling approach does not explicitly take into account the nature of the free counterions. Therefore, it may not be valid in this particular case if counterions have some additional influence. This influence could act on macroion interactions, through the electrostatic screening, or on the average conformation of the macroions. There is more reliable information on the second, which we discuss now.

5.3.2. Conformational Changes. So far, we have considered that the only effect of the counterions was a modification of the charge fraction. However, a counterion-induced attraction between monomers may also occur.[9,10,14,31] Such a phenomenon that is more pronounced with divalent counterions could be responsible for a retraction of the macroions. Then, the shift in q^* for pure CaPSS would be due to a collapse of the macroions, which in turn induces additional condensation and thus a decrease in the effective charge fraction. Neutron scattering measurements of the radii of gyration of NaPSS and CaPSS polyelectrolytes have been carried out by use of the zero average contrast (ZAC) method.[16,17] They show that the macroions related to CaPSS samples were shrunk with respect to those associated with NaPSS samples (R_g ratio of the order of 1.5−2). The scaling approach cannot account for such a difference via a charge renormalization according to the Manning−Oosawa theory alone. This implies that the overlap concentration c^* will not be correctly evaluated for CaPSS samples. More generally, the slightly collapsed conformation through Ca bridges should: first, enhance the counterion condensation process; second, lead to a higher c^* value that shifts the scattering peak toward lower q values and changes the exponent in the c dependence of the correlation length ξ.

Now, one has to explain why a shrinking of macroions is only observed for $X = 0$ (pure CaPSS) and not for $X = 0.25$ or for the other Na−CaPSS mixtures in which divalent counterions are also condensed ($X < 1$). At this stage we wish to emphasize that a similar effect is contained in the SANS study of Dubois et al.[17] As just said, for pure CaPSS solutions without any added salt, the average conformation of macroions cannot be fitted to the wormlike chain model, indicating a more shrunk conformation. But under addition of $CaCl_2$ to NaPSS solutions, the chain conformation can still be viewed as wormlike, as long as the $CaCl_2$ added salt concentration is low enough (the persistence length of the macroions decreases when the ionic strength is increased as usual). The role of the salt is out of the scope of that paper, but we can consider in a first approximation that part of the added Ca cations replace the initially monovalent condensed counterions while another part is scattered in the aqueous solution with the Na counterions. Therefore, solutions with low added salt concentration correspond to our X range, $0.25 \leq X < 1$ (no free divalent counterions), whereas large concentrations correspond to $X < 0.25$ (free divalent counterions). We see that here also aqueous solutions with free Ca counterions only exhibit the conformational shrinking, in agreement with our measurements.

It is remarkable that this chain retraction is just observed as free Ca counterions are free in the solution. It is also paradoxical because one electrostatic link should be more easily formed from a divalent counterion closely localized to at least one part of the chain, leading to a charge reversal. However, the coincidence of the chain shrinking with the presence of free Ca counterions in the solution may be not fortuitous. Actually, electrostatic bridges or loops, if they exist, could only be formed through some exchanges between condensed and free counterions. Since in addition divalent counterions have to be involved in such processes, the condition $X < 0.25$ (or 0.18) is then required.

To proceed further in this debate would be facilitated by numerical simulations. Few have been performed on flexible polylectrolytes in the presence of multivalent counterions. They indicate shrinkage in the macroion conformation.[25,42] Specifically, they enlighten the existence of intramolecular bridges formed by divalent counterions. They consider the macroion partial scattering function that exhibits a broad maximum whose the position q^* depends on the charge fraction.[25] In the dilute regime, q^* is found to be identical for monovalent and divalent counterions (for all charge fractions) and scales as $c^{1/3}$. In the semidilute regime, q^* is found to scale as $c^{1/2}$ for both counterion valences $Z = 1$ and 2, but the prefactor is found to vary with Z and the charge fraction. For divalent counterions, the prefactor is lower than for monovalent counterions. Numerical simulations are therefore in agreement with our measurements in the low concentration regime. Moreover, they show that a master curve can be obtained by rescaling q^* as a function of c/c^*. Thus, everything is correlated to a change in c^*, or in the average size of the macroions, when monovalent counterions are replaced by divalent ones. The origin of the shift in q^* for $X = 0$ is therefore related to a shrinkage in the macroion conformation due to an electrostatic bridging phenomena via Ca counterions. It must be noticed that even if these simulations capture the main characteristics of the effect of the counterion valence on the structure of the macroions, they are restricted to very short macroions.

5.4. High Concentration Regime. At higher concentrations, neither the scaling approach nor the numerical simulations are able to explain the q^* deviations with respect to the $c^{1/2}$ scaling law, observed for CaPSS and Na−CaPSS mixtures. In this concentration range, the nature of the condensed counterions is believed to play a relevant role in the structure of the solutions. As discussed previously, these deviations are probably related to the misunderstanding with the peak position that results from the influence of the counterion form factor upon the total scattering function measured by SAXS, as demonstrated for monovalent counterions in section 4.3. However, since the relative importance of this scattering effect on the q^* deviation is difficult to determine, other origins may be introduced.

The origin could also be a progressive increase in the counterion condensation related to the presence of divalent counterion and leading to a continuous decrease in the effective charge fraction.[20,74] For the highest concentrations, the scattering peak also disappears ($X = 0$, 0.25, and 0.5) and the scattering curves become similar to those of neutral polymers. Both the decrease in the scaling exponent for $c > 0.1$ mol/L and the disappearance of the scattering peak at higher concentrations are presumably correlated or could have the same origin.

Because such deviations resemble the ones observed for hydrophobic polyelectrolytes,[52−54,63,64,71,76] we checked the possible existence of hydrophobic microdomains in CaPSS and Na−CaPSS aqueous solutions using fluorescence spectroscopy (see Appendix B). The answer is negative: the observed deviations do not seem to be correlated to any hydrophobic effect.

In the case of pure CaPSS, divalent Ca counterions induce the formation of intramolecular bridges and thus a slight collapse that could mimic the one of a polyelectrolyte in poor solvent conditions. Also, the number of Ca bridges could vary with the concentration (as well as the effective charge fraction) and cause deviation from the $c^{1/2}$ scaling law.

As mentioned above, in this concentration range, the structure of the solutions is highly sensitive to the nature of condensed counterions. In the previous part of this work, we emphasized the importance of the free divalent counterions in the bridging process. Bridging phenomena observed for pure CaPSS could be enhanced at high concentration due to the reduction of the persistence length. This kind of interaction could also be conceivable for other mixtures even in the absence of free divalent counterions, provided that the concentration is high enough.

6. Summary and Conclusion

This study brings some new insights for understanding the so-called "polyelectrolyte peak" encountered in the small-angle scattering from salt-free polyelectrolyte solutions, using the trick of mixing monovalent and divalent counterions. These insights mainly concern the position in the reciprocal space, q^*, of the broad maximum observed in the scattering profiles, first associated with an electrostatic correlation hole within the isotropic model.[48] We used both small-angle X-ray and neutron scattering techniques to investigate the structure of the salt-free aqueous solutions of sulfonated polystyrene (PSS) macroions in the presence of various mixtures of sodium (Na) and calcium (Ca) counterions. q^* has been studied as a function of X, which is related to the ratio of monovalent (sodium, Na) to divalent (calcium, Ca) counterions as well as of the concentration of macroions, c, and compared with the inverse of the correlation length ξ predicted by scaling theories.[48−50]

One of the most relevant parameters shows to be the degree of condensation of counterions, successfully evaluated according to the Manning−Oosawa approach.[40,41]

First, we have reviewed the case of monovalent counterions by a survey of the literature which completes our measurements for the case $X = 1$ (i.e., pure NaPSS). We show that a universal curve exists, linking q^* and $2\pi/\xi$, not only for weakly charged polyelectrolytes but also for highly charged ones, provided one introduces an effective charge fraction estimated from the Manning−Oosawa approach of counterion condensation. In practice, the charge fraction f should only be replaced by the effective charge fraction $f_{\text{eff}} = b/l_B$, in the scaling law for the correlation length ξ as a function of f and concentration c:

$$\xi = f^{-2/7}(l_B/b)^{-1/7}(bc)^{-1/2}$$

(in which l_B and b are the Bjerrum and monomer lengths, respectively; we are here in the strong-coupling limit, since some of the counterions are bound or the counterion concentration in the vicinity of the macroions is finite). Conversely, information about the condensation of the monovalent counterions could be gained from q^* measurements for salt-free aqueous solutions.

Such relation as $q^* = 2\pi/\xi$ is surprisingly perfectly obeyed in a lower concentration range.

However, slight deviations from this equality (hence from the usual $c^{1/2}$ scaling law), which gradually increase with c, can be observed beyond a certain c or q^* value. The contrast with the good agreement at low c prompted us to a better understanding. It turns out that the relevant maximum is the one of the macroion partial

intermolecular scattering function, while the total scattering function can be affected by a slight change in the form factor.[75] The total scattering function involves intra- and intermolecular correlations as well as macroion and counterion partial scattering functions. Discrepancies are expected, all the more important as the counterion part of the scattering function is large (e.g., metal counterions for X-rays) and as the concentration increases (because q^* enters a higher q range with higher contribution of the counterion part). This could explain why the exponent of the scaling law linking q^* to c is found to vary from 0.46 to 0.5 in the literature (in good solvent), according to the scattering technique (X-ray or neutron), the nature of the counterions, the macroions, and the solvent.

Second, we used our results to show that this scaling−condensation model applies when monovalent (Na) counterions are replaced by divalent (Ca) ones, up to a certain fraction of Ca counterions. The same PSS macroion was considered; this is a model case because of the absence of complexation between macroion and counterions.

Following the Manning−Oosawa approach for the counterion condensation process, when X is varied from 1 (pure NaPSS) to 0 (pure CaPSS), three distinct X regimes are expected (Figure 5a). For low X values ($X < 0.18$), only Ca counterions are condensed and free counterions are composed of Na and Ca counterions. The effective charge fraction f_{eff} is then constant. In a particular X range ($0.18 < X < 0.36$), all Ca counterions are condensed and all Na counterions are free. In this regime, f_{eff} just scales as X. Finally, for high X values ($X > 0.36$), condensed counterions consists of both Na and Ca counterions, and there is a constant number of Na free counterions. Again, f_{eff} is constant.

In the low concentration range, the measured q^* values were found to be in qualitative agreement with such a description. In the range $X \geq 0.25$ (the theoretical limit is actually 0.18), everything seems to be governed by the valence of the free counterions (monovalent). That of the condensed counterions does not appear to be essential: changes in the static structure are described by changes in the effective charge fraction alone. This is supported by the existence of a master curve connecting q^* and $2\pi/\xi$.

Third, we have characterized deviations from the scaling model for larger fractions of divalent (Ca) counterions. For $X < 0.25$ (the theoretical limit is still 0.18), i.e., when Na free counterions are also replaced by Ca counterions or as part of Ca counterions are free, a more significant change in the structure is observed that cannot be accounted for by a simple charge renormalization. Specifically, for $X = 0$ the variations of q^* with c and f can no longer be described by the previous scaling law, even if one includes the counterion condensation according to the Manning−Oosawa approach. Obviously, the counterion condensation is not the only process.

We then have turned our interest toward the influence of divalent counterions on the macroion conformation, as already investigated by use of the zero average contrast (ZAC) method in SANS from aqueous solutions of CaPSS, as well as NaPSS plus added Ca salt.[16,17] The main effect is a retraction of the macroions that, in particular, modifies the scaling account for c^*. This retraction can be due to the existence of pure electrostatic Ca bridges between monomers apart from one another along the chemical sequence, i.e., the formation of temporary loops in the conformation. Such a conjecture seems to be quite reasonable, since it is in accordance with previous form factor measurements and simulations.[16,17,25] One has, however, still to derive a deeper theoretical description, especially allowing to precise the respective roles of free and condensed counterions. Finally, let us note that we have chosen not to discuss the effect of Ca free counterions on the Debye screening length because we do not expect it to be relevant in the investigated c range.

At this stage, we can conclude that divalent counterions are efficient in linking parts of chains only when a fraction of them is free (condensation has reached its maximum) which may seem surprising.

Fourth, when the concentration is increased, failures are present even for lower fractions of divalent (Ca) counterions. We have found that the scaling theory of Dobrynin, Colby, and Rubinstein, associated with the Manning−Oosawa approach of the counterion condensation, fails to explain our scattering results. Deviations from the usual $c^{1/2}$ scaling law are observed that enhance as the fraction of Ca counterions increases. Thus, the exponent of the scaling law linking q^* to c is reduced down to 0.2 as X is varied to 0. Also, the peak in the scattering function vanishes for $X = 0$, 0.25, and 0.5 above a certain concentration that increases with X. The role of the condensed divalent (Ca) counterions is clearly revealed. At this stage, such modifications are mainly due to the influence of the intramolecular correlations as in the case of monovalent counterions. However, a slight change in the condensation threshold is also conceivable. Bridging phenomena due to divalent counterions may also play a role even in absence of free divalent counterions, provided that the concentration is large enough. This high concentration regime also needs other investigations to be fully interpreted.

In summary, at low concentration, the scaling model for flexible polyelectrolytes in good solvent, combined with the Manning−Osawa estimation of the effective charge fraction, agrees with data for monovalent counterions alone or partly replaced by divalent ones, as long as those are all condensed on the macroions. When some divalent counterions are free, they introduce new interactions. At higher concentrations, these different effects may be even more intricate.

Acknowledgment. We thank Bruno Demé, from Institut Laue Langevin, and Fabien Schnell, from Institut Charles Sadron, for their help during neutron and X-ray small-angle scattering measurements. We are indebted to the Institut Laue Langevin for use of neutron beam time. Thanks are also due to Albert Johner for valuable discussions.

Appendix A. Condensation Process for Highly Charged Macroions in the Presence of Monovalent Counterions

The universal curve, linking q^* and $2\pi/\xi$, in Figure 6b does not correspond to a strict equality $q^* = 2\pi/\xi$, and deviations toward lower q^* values are observed beyond a certain c or q^* value. Actually, they are related to deviations from the usual $c^{1/2}$ scaling law, which gradually increase with c. As remarked in section 4.3, such deviations could be due to a progressive increase in the counterion condensation process, i.e., a continuous decrease in the counterion condensation threshold. The

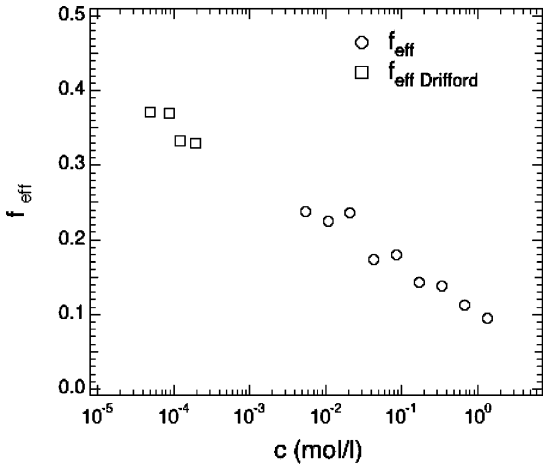

Figure 9. Effective charge fraction f_{eff} vs monomer concentration c for NaPSS. Here f_{eff} is an adjustable parameter derived from the scaling law (5′), by assuming that the q^* deviations from the strict equality $q^* = 2\pi/\xi$ in Figure 6b are exclusively due to an increase in the counterion condensation with c.

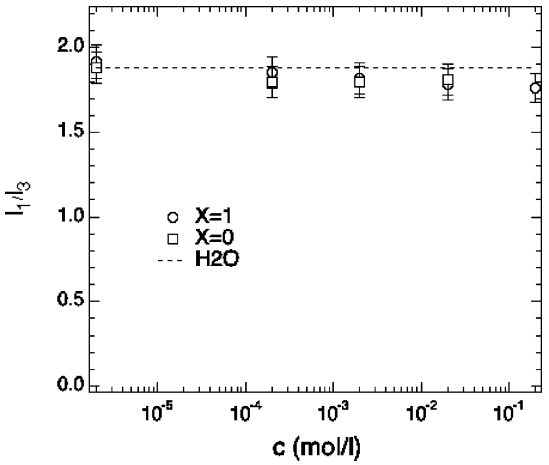

Figure 10. Ratio I_1/I_3 of the intensities of the first and third peaks of the fluorescence spectra of pyrene for pure NaPSS ($X = 1$) and CaPSS ($X = 0$) aqueous solutions at room temperature.

effective charge fraction would then be expected to vary with c. In this appendix, the effective charge fraction is considered as an adjustable parameter, and its c dependence is derived by using the scaling law (5′) as reference. We can emphasized that a comparison between q^* and $2\pi/\xi$ is not straightforward. A prefactor is indeed missing. Nevertheless, as suggested by the light scattering part of the master curve reported in Figure 6b, this prefactor should be close to unity. The results obtained from measurements on pure NaPSS samples are presented in Figure 9.

Whereas the effective charge fraction is close to 0.36 in the low concentration regime, i.e., the expected value according to the Manning−Oosawa theory, it is continuously reduced when the concentration is increased. This decrease is related to the fact that q^* does not rigorously follow the $c^{1/2}$ power law.

The effective charge fraction of fully sulfonated polystyrene has been measured by Essafi[53] and Baigl[71,81] using osmotic pressure and potentiometric techniques. The experimental value was found to be very close to the expected theoretical one (0.36) in the concentrations range 0.01−0.1 mol/L in contradiction with our extrapolations from the q^* measurements. If we cannot rule out a slight decrease of the effective charge fraction with the concentration, the departure to the $c^{1/2}$ power law in the q^* evolution or, in other words, the deviations from the strict equality $q^* = 2\pi/\xi$ has to be connected to another phenomenon.

Appendix B. Absence of Hydrophobic Microdomains in CaPSS Solutions

An increasing attention has been devoted to the properties of polyelectrolytes in poor solvent.[74,77−78] The macroions are expected to adopt a pearl-necklace conformation with dense charged aggregates (pearls) connected by stretched chain parts (narrow elongated strings).[77−79] In the semidilute regime, according to the concentration, two distinct scaling laws are then predicted for the c dependence of q^*. In the string controlled regime (c such as the distance between two successive beads along the chemical sequence is larger than ξ), q^* scales as $c^{1/2}$; in the bead-controlled regime (c such as this distance is less than ξ), it is a $c^{1/3}$ scaling law that prevails.[77] Some experiments on hydrophobic polyelectrolytes are in qualitative agreement with such a behavior.[52−54,64,71,76] The c dependence of q^* observed with fully sulfonated PSS macroions in the presence of mixed valence or divalent counterions has also a certain similarity and therefore could be related to a poor solvent effect or an hydrophobic character of the macroions. Partially sulfonated polystyrenes are hydrophobic polyelectrolytes of which the structure of their salt-free aqueous solutions has been extensively studied.[52,53,71,76] Such a hydrophobic character can be evidenced by studying: either the change in the scattered intensity by the aqueous solutions as the temperature is varied[53,54,80] or the fluorescence of pyrene molecules dissolved in the aqueous solutions.[53,71] This last method specifically allows to probe the existence of hydrophobic microdomains.

We also performed SAXS measurements on pure NaPSS and CaPSS at different temperatures. No major modification of the scattered intensity is observed as the temperature is varied from 20 to 80 °C. Such a behavior is quite different from the one of the aqueous solutions of partially sulfonated polystyrenes. We also made measurements on pure NaPSS in mixtures of water and THF (THF is a good solvent for polystyrene). A very slight displacement of q^* is observed that is only explained by a change in the dielectric constant. The Na−CaPSS mixtures can also be considered as hydrophilic, as dissolved in water.

This is still proved by measurements of the fluorescence of pyrene molecules. Indeed, if the pyrene molecules were trapped in hydrophobic microdomains, the ratio I_1/I_3 should be reduced. As shown in Figure 10, this is not the case since I_1/I_3 remains similar as Na counterions are replaced by Ca counterions and close to the value associated with pyrene molecules in pure water.

References and Notes

(1) Hara, M., Ed.; *Polyelectrolytes: Science and Technology*; Marcel Dekker: New York, 1993.
(2) Schmitz, K. S. *Macroions in Solution and Colloidal Suspensions*; VCH: New York, 1993.
(3) Förster, S.; Schmidt, M. *Adv. Polym. Sci.* **1995**, *120*, 51.
(4) Barrat, J.-L.; Joanny, J.-F. *Adv. Chem. Phys.* **1996**, *94*, 1.
(5) Radeva, T., Ed.; *Physical Chemistry of Polyelectrolytes*; Marcel Dekker: New York, 2001.

(6) Holm, C., Kekicheff, P., Podgornik, R., Eds.; *Electrostatic Effects in Soft Matter and Biophysics*; NATO Sci. Ser. II; Kluwer Academic Press: Dordrecht, 2001; Vol. 46.
(7) Widom, J.; Baldwin, R. L. *J. Mol. Biol.* **1980**, *144*, 431; *Biopolymers* **1983**, *22*, 1595.
(8) Bloomfield, V. A. *Biopolymers* **1991**, *31*, 1471; *Curr. Opin. Struct. Biol.* **1996**, *6*, 334.
(9) Huber, K. *J. Phys. Chem.* **1993**, 97, 9825. Ikeda, Y.; Beer, M.; Schmidt, M.; Huber, K. *Macromolecules* **1998**, *31*, 728.
(10) Axelos, M. A.; Mestdagh, M. M.; François, J. *Macromolecules* **1994**, *27*, 6594. Heitz, C. Thesis, Université Louis Pasteur de Strasbourg, 1996. François, J.; Heitz, C.; Mestdagh, M. M. *Polymer* **1997**, *38*, 5321. Heitz, C.; François, J. *Polymer* **1999**, *40*, 3331.
(11) Olvera de la Cruz, M.; Belloni, L.; Delsanti, M.; Dalbiez, J.-P.; Spalla, O.; Drifford, M. *J. Chem. Phys.* **1995**, *103*, 5781.
(12) Yoshikawa, K.; Takahashi, M.; Vasilevskaya, V. V.; Khokhlov, A. R. *Phys. Rev. Lett.* **1996**, *76*, 3029.
(13) Tang, J. X.; Janmey, P. A. *J. Biol. Chem.* **1996**, *271*, 8556. Tang, J. X.; Wong, S.; Tran, P.; Janmey, P. A. *Ber. Bunsen-Ges. Phys. Chem.* **1996**, *100*, 1. Tang, J. X.; Ito, T.; Tao, T.; Traub, P.; Janmey, P. A. *Biochemistry* **1997**, *36*, 12600.
(14) Sabbagh, I. Thesis, Université Paris VII, 1997. Sabbagh, I.; Delsanti, M.; Lesieur, P. *Eur. Phys. J. B* **1999**, *12*, 253. Sabbagh, I.; Delsanti, M *Eur. Phys. J. E* **2000**, *1*, 75. Drifford, M.; Delsanti, M. In *Physical Chemistry of Polyelectrolytes*; Radeva, T., Ed.; Marcel Dekker: New York, 2001; Chapter 4, pp 135−161.
(15) Raspaud, E.; Olvera de la Cruz, M.; Sikorav, J.-L.; Livolant, F. *Biophys. J.* **1998**, *74*, 381.
(16) Zhang, Y.; Douglas, J. F.; Ermi, B. D.; Amis, E. J. *J. Chem. Phys.* **2001**, *114*, 3299.
(17) Dubois, E.; Boué, F. *Macromolecules* **2001**, *34*, 3684.
(18) Wong, G. C. L.; Lin, A.; Tang, J. X.; Li, Y.; Janmey, P. A.; Safinya, C. R. *Phys. Rev. Lett.* **2003**, *91*, 18103. Butler, J. C.; Angelini, T.; Tang, J. X.; Wong, G. C. L. *Phys. Rev. Lett.* **2003**, *91*, 28301. Angelini, T. E.; Liang, H.; Wriggers, W.; Wong, G. C. L. *Proc. Natl. Acad. Sci. U.S.A.* **2003**, *100*, 8634.
(19) Sorci, G. A.; Reed, W. F. *Macromolecules* **2004**, *37*, 554.
(20) Stevens, M. J.; Kremer, K. *Phys. Rev. Lett.* **1993**, *71*, 2228; *J. Chem. Phys.* **1995**, *103*, 1669.
(21) Stevens, M. J. *Phys. Rev. Lett.* **1999**, *82*, 101.
(22) Gronbech-Jensen, N.; Mashl, R. J.; Bruinsma, R. F.; Gelbart, W. M. *Phys. Rev. Lett.* **1997**, *78*, 2477.
(23) Chu, J. C.; Mak, C. H. *J. Chem. Phys.* **1999**, *110*, 2669.
(24) Liu, S.; Muthukumar, M. *J. Chem. Phys.* **2002**, *116*, 9975.
(25) Chang, R.; Yethira, A. *J. Chem. Phys.* **2003**, *118*, 11315.
(26) Wittmer, J.; Johner, A.; Joanny, J.-F. *J. Phys. II* **1995**, *5*, 635.
(27) Gonzales-Mozuelos, P.; Olvera de la Cruz, M. *J. Chem. Phys.* **1995**, *103*, 3145.
(28) Rouzina, I.; Bloomfield, V. A. *J. Phys. Chem.* **1996**, *100*, 9977.
(29) Ha, B.-Y.; Liu, A. J. *Phys. Rev. Lett.* **1997**, *79*, 1289; *Phys. Rev. Lett.* **1998**, *81*, 1011; *Phys. Rev. E* **1998**, *58*, 6281; *Phys. Rev. E* **1999**, *60*, 803.
(30) Brilliantov, N. V.; Kuznetsov, D. V.; Klein, R. *Phys. Rev. Lett.* **1998**, *81*, 1433.
(31) Schiessel, H.; Pincus, P. *Macromolecules* **1998**, *31*, 7953.
(32) Golestanian, R.; Kardar, M.; Liverpool, T. B. *Phys. Rev. Lett.* **1999**, *82*, 4456.
(33) Kuhn, P. S.; Levin, Y.; Barbosa, M. C. *Physica A* **1999**, *266*, 413.
(34) Solis, F. J.; Olvera de la Cruz, M. *Eur. Phys. J. E* **2001**, *4*, 143.
(35) Solis, F. J. *J. Chem. Phys.* **2002**, *117*, 9009.
(36) Borukhov, I.; Lee, K.-C.; Gelbart, W. M.; Liu, A. J.; Stevens, M. J. *J. Chem. Phys.* **2002**, *117*, 462.
(37) Ermoshkin, A. V.; Olvera de la Cruz, M. *Phys. Rev. Lett.* **2003**, *90*, 125504.
(38) Ermoshkin, A. V.; Olvera de la Cruz, M. *J. Polym. Sci., Part B: Polym. Phys.* **2004**, *42*, 766.
(39) Naji, A.; Netz, R. R. *Eur. Phys. J. E* **2004**, *13*, 43.
(40) Manning, G. S. *J. Chem. Phys.* **1969**, *51*, 924, 934; *Annu. Rev. Phys. Chem.* **1972**, *23*, 117; *Ber. Bunsen-Ges. Phys. Chem.* **1996**, *100*, 909.
(41) Oosawa, F. *Biopolymers* **1968**, *6*, 134; *Polyelectrolytes*; Marcel Dekker: New York, 1971.
(42) Holm, C.; Kremer, K. *Proceedings of Yamada Conference L Polyelectrolytes*; Yamada Science Foundation: Osaka, 1999; p 27.
(43) Dolar, D.; Peterlin, A. *J. Chem. Phys.* **1969**, *50*, 3011.
(44) Dolar, D. In *Polyelectrolytes*; Sélégny, E., Ed.; Reidel Publishing: Dordrecht, 1974; pp 97−113.
(45) Rinaudo, M.; Loiseleur, B. *Bull. Soc. Chim.* **1973**, *124*, 1.
(46) Rinaudo, M. In *Polyelectrolytes*; Sélégny, E., Ed.; Reidel Publishing: Dordrecht, 1974; pp 157−193.
(47) Tomsic, M.; Bester Rogac, M.; Jamnik, A. *Acta Chim. Slov.* **2001**, *40*, 333.
(48) de Gennes, P.-G.; Pincus, P.; Velasco, R. M.; Brochard, F. *J. Phys. (Paris)* **1976**, *37*, 1461.
(49) Pfeuty, P. *J. Phys., Colloq.* **1978**, *C2*, 149.
(50) Dobrynin, A. V.; Colby, R. H.; Rubinstein, M. *Macromolecules* **1995**, *28*, 1859.
(51) Makowski, H. S.; Lundberg, R. D.; Singhal, G. S US Patent 3870841, 1975, to Exxon Research and Engineering Co.
(52) Essafi, W.; Lafuma, F.; Williams, C. E. In *Macroion Characterization from Dilute Solutions to Complex Fluids*; ACS Symposium Series 548; Schmitz, K. S., Ed.; American Chemical Society: Washington, DC, 1994; Chapter 21, pp 278−286.
(53) Essafi, W. Thesis, Université Paris VI, 1996.
(54) Heinrich, M. Thesis, Université Louis Pasteur de Strasbourg, 1998.
(55) Baigl, D.; Seery, T. A. P.; Williams, C. E. *Macromolecules* **2003**, *36*, 6878.
(56) Tondre, C.; Zana, R. *J. Phys. Chem.* **1972**, *76*, 3451.
(57) Millero, F. J. In *Water and Aqueous Solutions*; Horne, R. A., Ed.; Wiley-Interscience: New York, 1972; Chapter 13.
(58) Glatter, O., Kratky, O., Eds.; *Small-Angle X-ray Scattering*; Academic Press: London, 1982. Cotton, J.-P. In *Neutron, X-ray and Light Scattering: Introduction to an Investigate Tool for Colloidal and Polymeric Systems*; Lindner, P., Zemb, Th., Eds.; North-Holland Delta Series: Amsterdam, 1991; Chapter 2, pp 19−31. Lindner, P. In *Neutrons, X-rays and Light: Scattering Methods Applied to Soft Condensed Matter*; North-Holland Delta Series: Amsterdam, 2002; Chapter 2, pp 23−48.
(59) Sears, G. D. *Neutron News* **1992**, *3*, 26.
(60) El Brahmi, K. Thesis, Université Louis Pasteur de Strasbourg, 1991.
(61) Nishida, K.; Kaji, K.; Kanaya, T. *Macromolecules* **1995**, *28*, 2472.
(62) Ermi, B. D.; Amis, E. J. *Macromolecules* **1997**, *30*, 6937.
(63) Essafi, W.; Lafuma, F.; Williams, C. E. *Eur. Phys. J. B* **1999**, *9*, 261.
(64) Waigh, T. A.; Ober, R.; Williams, C.; Galin, J.-C. *Macromolecules* **2001**, *34*, 1973.
(65) Drifford, M.; Dalbiez, J.-P. *J. Phys. Chem.* **1984**, *88*, 5368.
(66) Cotton, J.-P.; Moan, M. *J. Phys., Lett.* **1976**, *37*, L-75.
(67) Nierlich, M.; Williams, C. E.; Boué, F.; Cotton, J.-P.; Daoud, M.; Farnoux, B.; Jannink, G.; Picot, C.; Moan, M.; Wolf, C.; Rinaudo, M.; de Gennes, P.-G. *J. Phys. (Paris)* **1979**, *40*, 701.
(68) Ise, N.; Obuko, T.; Kunugi, S.; Matsuoka, H.; Yamamoto, K. I.; Ishii, Y. *J. Chem. Phys.* **1984**, *81*, 3294.
(69) Kaji, K.; Urakawa, H.; Kanaya, T.; Kitamaru, R. *J. Phys. (Paris)* **1988**, *49*, 993.
(70) Manning, G. S. In *Polyelectrolytes*; Sélégny, E., Ed.; D. Reidel: Dordrecht, 1974; pp 9−37.
(71) Baigl, D. Thesis, Université Paris VI, 2003.
(72) Reddy, M.; Marinsky, J. A.; Sarkar, A. *J. Phys. Chem.* **1970**, *74*, 3891.
(73) Hayter, J.-B.; Jannink, G.; Brochard-Wyart, F.; de Gennes, P.-G. *J. Phys., Lett.* **1980**, *41*, L-451.
(74) Micka, U.; Holm, C.; Kremer, K. *Langmuir* **1999**, *15*, 4033.
(75) Nishida, K.; Kaji, K.; Kanaya, T.; Shibano, T. *Macromolecules* **2002**, *35*, 4084.
(76) Baigl, D.; Ober, R.; Qu, D.; Fery, A.; Williams, C. E. *Europhys. Lett.* **2003**, *62*, 588.
(77) Dobrynin, A. V.; Rubinstein, M.; Obukhov, S. P. *Macromolecules* **1996**, *29*, 2974. Dobrynin, A. V.; Rubinstein, M. *Macromolecules* **1999**, *32*, 915.
(78) Limbach, H. J.; Holm, C.; Kremer, K. *Europhys. Lett.* **2002**, *60*, 566.
(79) Kantor, Y.; Kardar, M. *Europhys. Lett.* **1994**, *27*, 643. Kantor, Y.; Kardar, M. *Phys. Rev. E* **1995**, *51*, 1299.
(80) Boué, F.; Cotton, J.-P.; Lapp, A.; Jannink, G. *J. Chem. Phys.* **1994**, *101*, 2562.
(81) Qu, D.; Baigl, D.; Williams, C. E.; Möhwald, E.; Fery, A. *Macromolecules* **2003**, *36*, 6878.
(82) Shew, C. Y.; Yethiraj, A. *J. Chem. Phys.* **1999**, *110*, 11599.

MA0479722